

# ANALYSIS OF FLIGHT CHARACTERISTICS OF PAPER AIRPLANES

Md Hasibuzzaman, Md Kamrul Hasan  
 Department of Mechanical Engineering  
 Rajshahi University of Engineering & Technology  
 Rajshahi-6204, Bangladesh

**Abstract:** The trajectory of a paper airplane is dependent on its lift and drag performance and aerodynamic stability. Historically, darts were the perfect choice for distance competitions because of their excellent stability, but John Collins has changed this tradition with his incredible design, Susanne, by making a new distance record in 2012. In this paper, differences between this world record design and other typical paper airplanes are represented using typical models of a dart and glider since the wingspan of Susanne fits in between them. Solid models of these three airplanes are created with Solid Works and analyzed with ANSYS Fluent at different attack and sideslip angles. Finally, a comparison is made considering lift, drag, and aerodynamic stability. From the simulated results, it is observed that Susanne performed moderately in terms of lift and drag performance and yaw stability; however, it possesses the maximum amount of roll stability.

**Keywords:** Angle of attack, Sideslip angle, Aerodynamic stability.

## I. INTRODUCTION

The art of paper folding, or origami, evolved and became popular within a century of the invention of paper (500 BCE). The first folded paper glider was developed in this period somewhere in ancient China or Japan. Since then, paper airplanes have been used to understand the properties of air and airborne objects [1]. Even the forefathers of modern flight used paper model aircraft to develop their designs. Though airplane manufacturers do not use paper-made models anymore, these models still play a vital role in the study of Micro Air Vehicles (MAV), and it goes without saying that paper airplanes are still used as fascinating toys [2]. Consequently, different competitions are arranged for paper airplanes all over the world, focusing on two parameters of flight: distance and time. In this paper, the differences between the current distance record-achieving model and two other typical paper airplane models are revealed using CFD simulation [3].

## II. CONSTRUCTION

The world record model Susanne is made with an 8.5" by 11" paper sheet, and the wingspan of this model is a bit wider than

a dart but narrower than a glider. So, to make a perfect comparison, both of the dart and glider models are made with paper sheets of the same dimension. The relevant dimensions of these airplanes are given in Table I.

Table-1: Basic dimensions

Name of the model	Wingspan (cm)	Wing height (cm)	Wing area (sq cm)
Susanne	19.9	19.1	147
Typical dart	14.48	29	169.2
Typical glider	19.65	14.3	229

The construction procedure of these three models is shown in Figure 1.

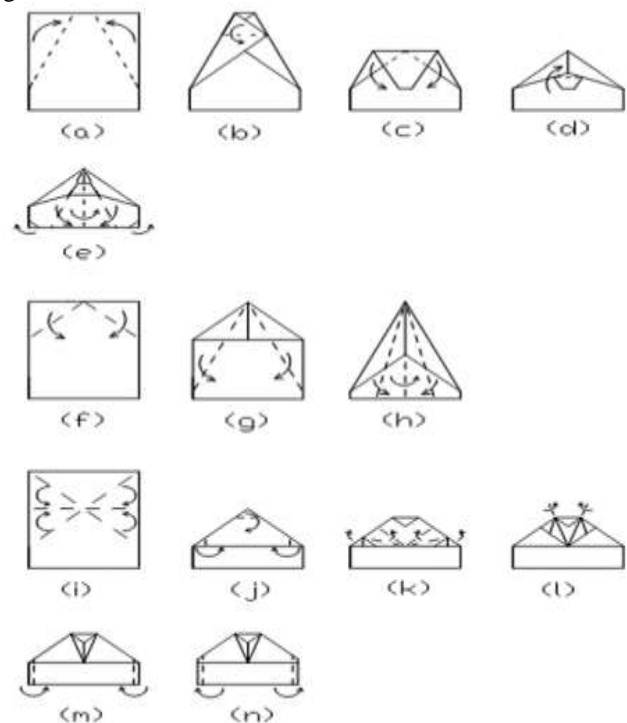


Fig.1. Construction procedure of Susanne (a-e), typical dart (f-h), and typical glider (i-n).

It is observed from practical experience that long origami structures always tend to deform a bit when sharp creases are

made. So, for each of these models, a certain amount of distance is observed between the upper and lower layers of the wings. 3D designs made by different modelling software by folding rectangular sheets are not helpful in imitating this practical issue [4]. As a result, solid models are created using Solid Works to attain better accuracy. John Collins designed his model with a positive dihedral angle to attain better lateral stability. With the increase in dihedral angle, lift-generating capacity decreases. So, the dihedral angle should not be very high either. The solid models of Susanne and the typical dart are designed with a 20° dihedral angle [7]. Since there is no centrefold in the glider, it is practically impossible to introduce any dihedral angle in this model. The solid models created by SolidWorks are shown in Figure 2.

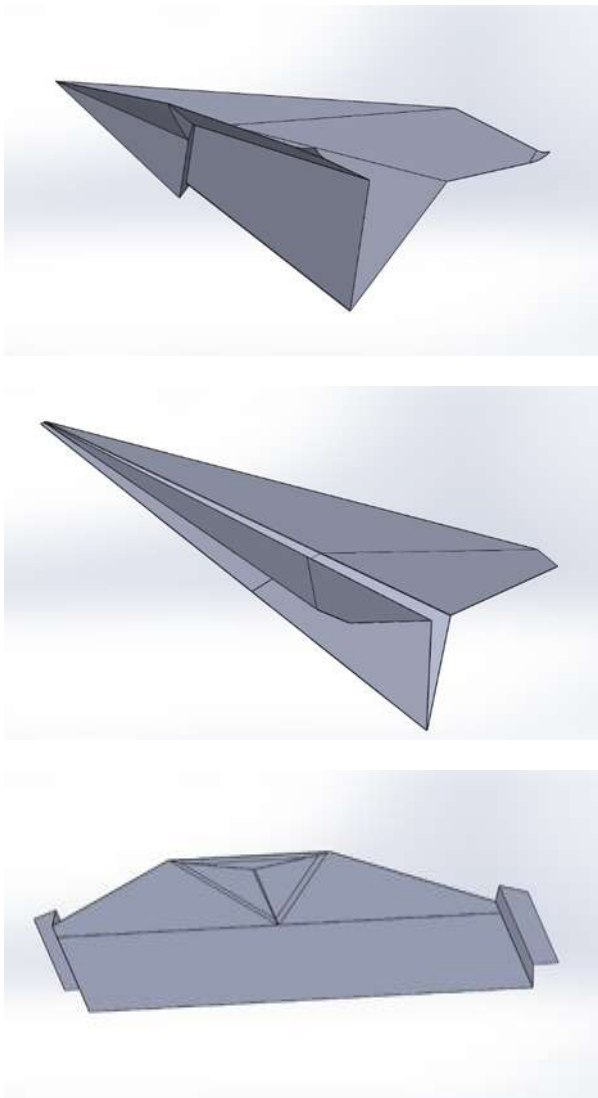


Fig.2. 3D model of Susanne, typical dart, and typical glider (from top to bottom).

### III. SIMULATION SETUP

Sufficiently spacious fluid domains (about 25 cm in the upstream region and about 45 cm in the downstream region) are created to get better results. A sample of a fluid domain is shown in Figure 3. A mesh independence study is performed, considering the coefficient of lift as a variable [6].

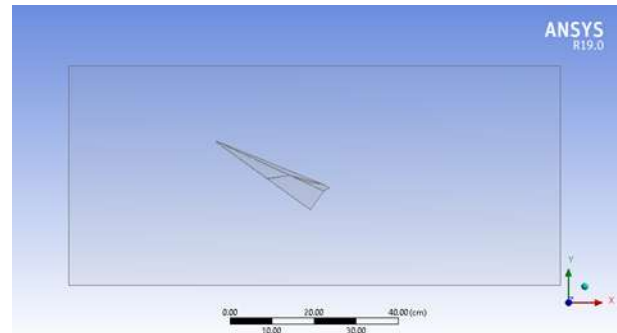


Fig.3 Fluid domain of typical dart.

From Figure 4, it can be seen that seven simulations are carried out in this process. The difference between the last four values is within the 3% tolerance limit [8]. So, the mesh that produces 3.5 million elements is chosen.

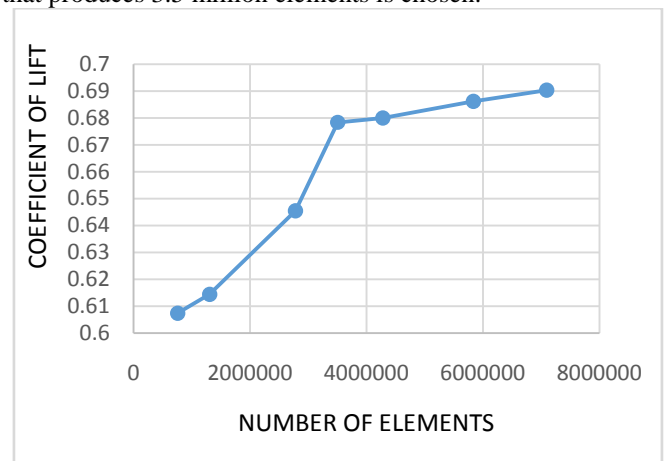


Fig.4. Mesh independence study.

Unstructured mesh is used for simplicity. More information about meshing is given below in table II.

Table-2: Mesh setup.

<b>Face sizing</b>	0.001m
<b>Number of inflation layers</b>	15
<b>Growth rate</b>	1.2
<b>Max face size</b>	0.01m

To get better results, meshing is performed separately for each of these angles mentioned before. A sample of the generated

mesh in the cross-section of the left wing of a typical dart is shown in Figure 5.

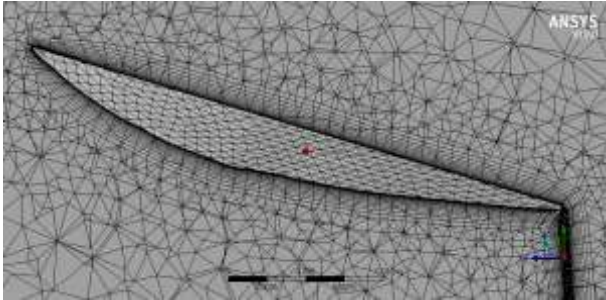


Fig.5.Mesh generated at the cross-section of the left wing of typical dart.

ANSYS A fluent solver is used to run these CFD simulations. To conduct an accurate simulation, several factors have been taken into consideration. Inlet airspeed is kept at 5 m/s for each of these simulations to avoid the issue of flutter [10]. Boolean is chosen during the creation of the fluid domain to subtract the internal volumes of these models from the surroundings to attain simplicity. For the lift and drag related simulations, the angles of attack are changed from 0° to 30° with an interval of 10° and from 30° to 50° with an interval of 5° to find out the exact angle of attacks for stall conditions. Similarly, stability-related simulations are run with a 5° sideslip angle interval. The turbulent model is selected according to the simulations carried out by NG et al. [9]. The solutions are generally converging on the boundary conditions of the solver, which are given below in Table III.

Table-3: Solver setup

<b>Velocity of flow</b>	5m/s
<b>Time</b>	Steady
<b>Pressure</b>	1 atm
<b>Turbulent model</b>	Spallart-Allmaras (1 eqn)
<b>Wall roughness constant</b>	0.5
<b>Fluid</b>	Air
<b>Density of fluid</b>	1.225 Kg/m <sup>3</sup>
<b>Viscosity</b>	1.7894e-5 Kg/m-s

To obtain accurate values, iterations are continued until the values stabilize. Figure 6 represents the output of the coefficient of lift of Susanne at 40° AOA.



Fig.6. Coefficient of lift of Susanne at 40° AOA

#### IV. ANALYSIS OF LIFT AND DRAG COEFFICIENTS

It is a common practice to use the lift and drag coefficients of an aircraft to analyze its flight performance. Mathematically, lift and drag coefficients are expressed in following equations [4].

$$C_L = \frac{2F_L}{\rho V^2 A} \quad (1)$$

$$C_D = \frac{2F_D}{\rho V^2 A} \quad (2)$$

Where,

Reynolds number, density of fluid(kg/ m<sup>3</sup>), inlet air velocity(ms-1), height of the wings(m), dynamic viscosity(kg/ms), coefficient of lift, coefficient of drag, lift force, drag force, surface area are expressed by Re, ρ, V, D, μ, C<sub>L</sub>, C<sub>D</sub>, F<sub>L</sub>, F<sub>D</sub>, A gradually.

Figure 7 shows that, for each of these models, the coefficient of lift increases with the increment of the angle of attack. However, at a certain angle (around 35° AOA), stalling occurs in all of these models, and the coefficient of lift starts to fall. At a 0° angle of attack, lift generated by the glider and the dart is nearly zero, but due to the aligned lower portion of Susanne, it is capable of generating a significant amount of lift at this position. On the other hand, from Figure 8, it is clear that coefficients of drag increase slowly with angle of attack and exhibit rapid growth after a while. Besides, from Figure 9 it is calculated that the values of the maximum lift-drag ratio for dart, Susanne, and glider are 3.31, 3.95, and 5.08, respectively, and the optimum angle of attack for dart and glider is nearly 10°, whereas for Susanne this angle is 0°. In addition, it is observed that, at the maximum lift-drag ratio point, the typical glider model possesses the highest amount of lift in relation to drag. The typical dart model, on the other hand, can achieve the least amount of lift among these models.

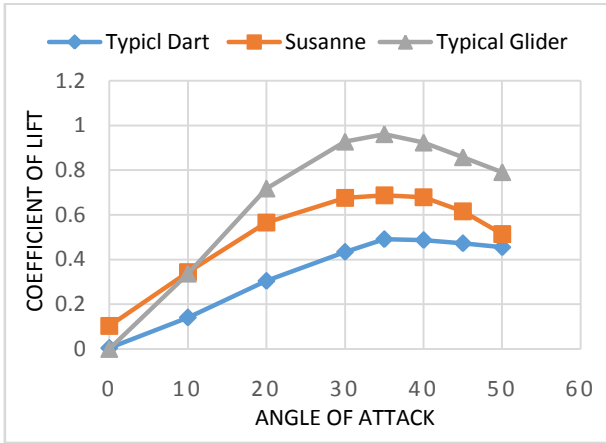


Fig.7. Lift curves of paper airplane models

The density and dynamic viscosity of air in this case are 1.225 kg/m<sup>3</sup> and 1.7894 kg/m<sup>3</sup>, respectively. According to equation 3, the relevant Reynolds numbers for the dart, Susanne, and glider are 99265, 65378, and 48947, respectively. From the experiments of Chen and Lie [11], it is seen that for the models of similar Reynolds numbers, the relevant values (maximum lift-drag ratio, angle of stall, and optimum angle of attack) are similar. To represent the properties of the fluid domains of these models at the maximum lift-drag ratio point, relevant figures of pressure contours are given below. Pressure contours are created at the midsection of the left-wing of each airplane and shown in Figure 10, Figure 11, and Figure 12. From these figures, the difference in pressure generated between the upper and lower surfaces of the wings can be observed.

Using the values of the lengths of these paper airplanes (Table 1) and flight speeds (5 m/s), relevant Reynolds numbers are obtained from the following equation,

$$Re = \frac{\rho V D}{\mu} \quad (3)$$

Where, Reynolds number, density of fluid(kg/ m<sup>3</sup>), inlet air velocity(ms-1) ,height of the wings(m), dynamic viscosity(kg/ms)are expressed by Re ,ρ, V, D, μ, gradually.

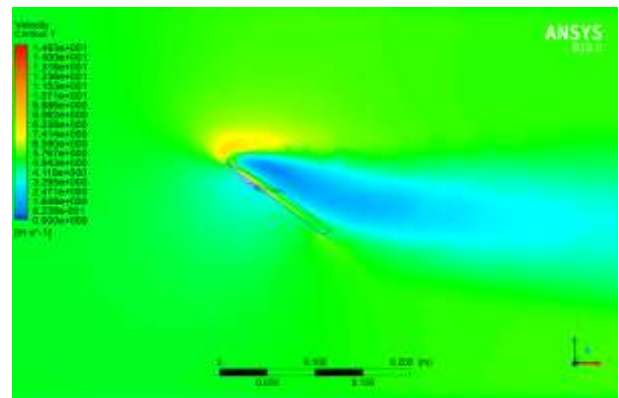


Fig.10. Velocity contour of Susanne at 35° AOA.

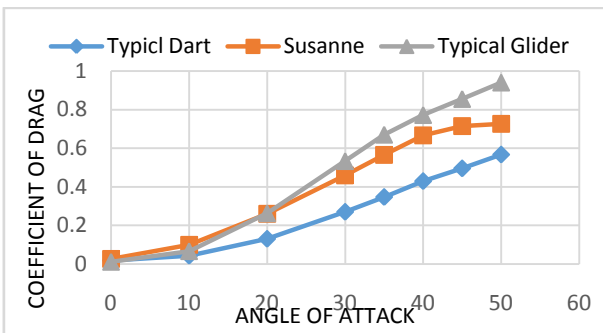


Fig.8. Drag curves of paper airplane models.

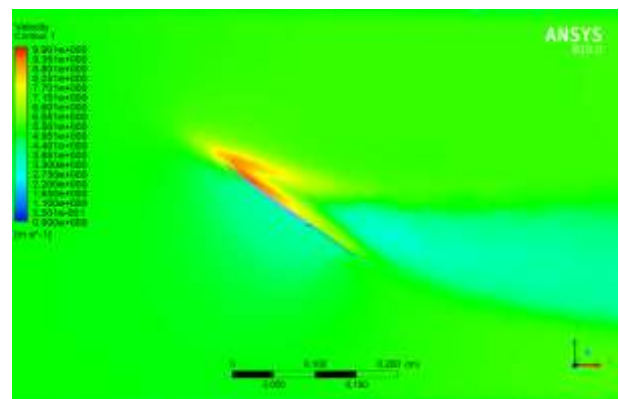


Fig.11. Velocity contour of typical dart at 35° AOA

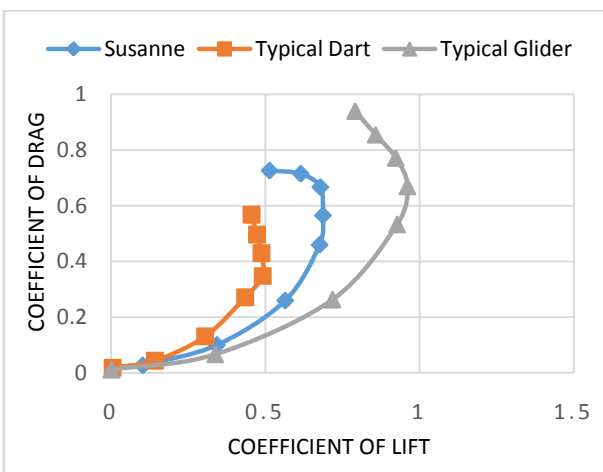


Fig.9. Drag vs lift curves.



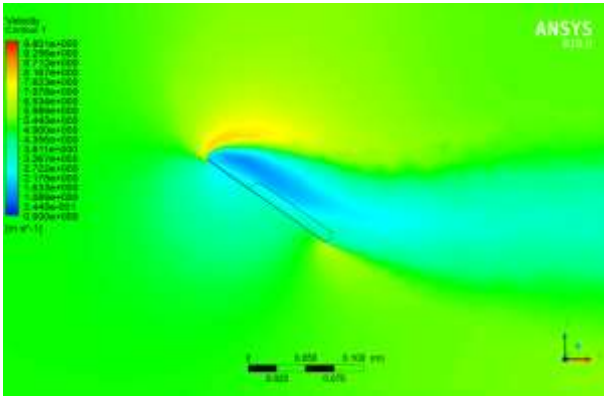


Fig.12. Velocity contour of typical glider at 35° AOA.

### V. ANALYSIS OF AERODYNAMIC STABILITY

Like all other actual airplanes, paper airplanes represent three basic types of movements with respect to the X, Y, and Z axes. These movements are named as pitch, roll, and yaw respectively. The moments and moment coefficients associated with these three axes, explain the characteristics of the stability of an aircraft. In this paper, analysis of aerodynamic stability is conducted according to the procedure of Nguyen et al. [6]. All the stability related simulations are performed at 0° AOA at different sideslip angles [5].

According to the angle convention, a negative yawing moment is generated by the relative wind when an aircraft flies with a positive sideslip angle. To bring back stability (to make the fuselage aligned with the direction of the relative wind), a net positive restoring yawing moment is needed. For positive sideslip angles, the higher the value of the positive yawing moment, the higher the degree of yaw stability[12]. The yawing moment coefficient is represented in the following equation

$$C_n = \frac{2N}{\rho V^2 S b} \quad (4)$$

Where,  $C_n$ = rolling moment coefficient,  $L$ = rolling moment,  $N$ = yawing moment,  $b$ = wingspan,  $S$ = wing area

Figure 13 represents the yawing moment coefficients of these paper airplanes with respect to the sideslip angle. From Figure 13, it can be seen that the typical dart is the most directionally stable model because of the huge centerfold, which acts as a radar. Susanne's yaw stability performance is quite similar to the dart just because of the presence of the centerfold, though it is not that stable. At a 10° sideslip angle, its yawing moment coefficient is 21.89% lower than that of a dart. On the other hand, a typical glider possesses the lowest amount of yaw stability with the lowest yawing moment coefficient, which is 82.16% lower than Susanne at a 10° sideslip angle.

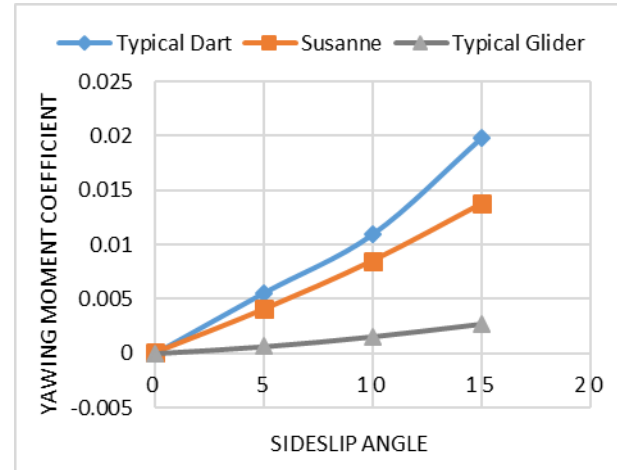


Fig.13. Yawing moment coefficient vs sideslip angle

To achieve roll stability, the values of the rolling moment coefficient should be as negative as possible while increasing the positive sideslip angle. The rolling moment coefficient is expressed in equation (5).

$$C_l = \frac{2L}{\rho V^2 S b} \quad (5)$$

$C_l$ = Yawing moment coefficient,  $L$ = Rolling moment,  $N$ = Yawing moment,  $b$ = Wingspan,  $S$ = Wing area

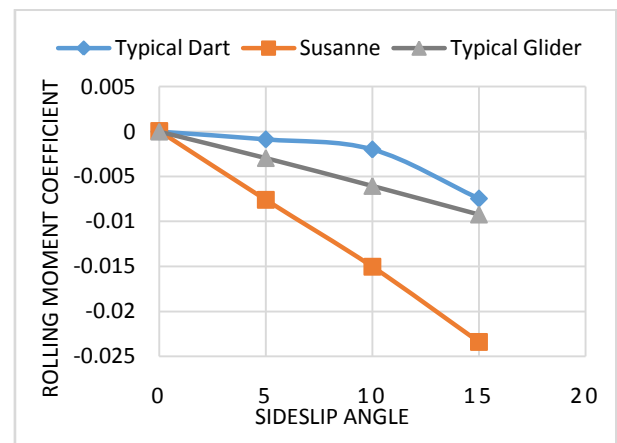


Fig.14. Rolling moment coefficient vs sideslip angle

Figure 14 depicts the rolling moment coefficients of these models for different sideslip angles. This figure shows that Susanne possesses the best roll stability among these models, followed by the typical glider and the typical dart. Susanne's rolling moment coefficient is 59.72% lower than that of a typical glider and 86.85% lower than that of a typical dart at a 10° sideslip angle. It is clear that Susanne possesses excellent roll stability because the wings are attached to the fuselage with a positive dihedral angle and because of the moderate length of the wingspan. Though the typical dart model is also designed with the same dihedral angle as Susanne, its wingspan is the shortest among these three models and it possesses the lowest amount of roll stability.



## VI. CONCLUSION

After the analysis of lift and drag performance and aerodynamic stability, the differences between these three paper airplanes can be easily observed. Though the typical dart model holds the lowest lift-drag ratio, it shows the maximum amount of yaw stability. Because of these reasons, darts can follow a smooth trajectory and travel a moderate amount of distance. The typical glider model is best at generating lift in terms of drag, but it shows considerably poor performance in terms of stability, like all other paper gliders. As a result, gliders are not so good at traveling linearly, but they represent excellent performance for being airborne for a long time. Finally, it goes without saying that Susanne is the most optimistic model to break a distance record. Though this model's lift-drag ratio at the optimum angle of attack position is 46.26% lower than the glider and 17.86% higher than the dart, it represents excellent yaw stability and the best roll stability among these models. All of these factors contributed to this model setting a Guinness World Record for distance.

## VII. REFERENCES

- [1]. Teran, F. J. L., and Rodriguez. (2016). Performance improvement of a 500-KW Francis turbine based on CFD, *Renewable Energy*, (pp. 977-992).
- [2]. Cook.(2017). Experimental analysis of paper plane flight characteristics, The University of Queensland
- [3]. NG, Y. Y. P., and Schluter. (2009).On the aerodynamics of paper airplanes, 27th AIAA Applied Aerodynamics Conference, AIAA 2009-3958.
- [4]. Uddin, M. Z. I., M. R., and Rubel. (2015). Experimental and numerical measurement of lift and drag force of NACA 0015 airfoil blade, *International Conference Mech. Ind. Mate. Engg.*
- [5]. Chen, K. and Lai, W. (2013). Paper plane aerodynamics, Xiamen Foreign Language School, ID: 1310, (pp- 22).
- [6]. Kim, W., Choi, W., Nguyen, N., Lee, J., Kim, S., Byun, Y., and Sur, J.M. (2010). Stability analysis of full geometry aircraft through CFD and response surface method, 48th AIAA Aerospace Sciences Meeting Including the New Horizons Forum and Aerospace Exposition, doi.org/10.2514/6.2010-1434.
- [7]. Mueller T. (2001). An Overview of Micro Air Vehicle Aerodynamics, in *Fixed and Flapping Wing Aerodynamics for Micro Air Vehicle Applications*, AIAA, Progress in Astronautics and Aeronautics, (pp. 1-10)
- [8]. Jones, K., Duggan, S. J., and Plazer. M. F (2001). Flapping Wing Propulsion for a Micro Air Vehicle, in 39th Aerospace Sciences Meeting and Exhibit.
- [9]. Mueller, T., Kellogg, J., Ifju, P., Shkarayev, S.(2006).Introduction to the Design of Fixed Wing Micro Air Vehicles, AIAA Education Series.
- [10]. Platzer, M., and Jones K. (2006). Flapping Wing Aerodynamics – Progress and Challenges, 44th Aerospace Sciences Meeting and Exhibit. 2006.
- [11]. Traub , L.W., Moeller, Brian, Rediniotis(1998). Othon, Low-Reynolds-Number Effects on Delta-Wing Aerodynamics. *Journal of Aircraft*, (pp. 653-656).
- [12]. Wentz, W.H.K., D. L. (1971). Vortex breakdown on slender sharp-edged wings *Journal of Aircraft*, (pp. 156-161).